Defence Science Journal, Vol. 55, No. 1, January 2005, pp. 21-36

Hydrodynamic Design of Integrated Bulbous Bow/Sonar Dome for Naval Ships

R. Sharma and O.P. Sha

Indian Institute of Technology Kharagpur, Kharagpur–721 302

ABSTRACT

Recently, the idea of bulbous bow has been extended from the commercial ships to the design of an integrated bow that houses a sonar dome for naval ships. In the present study, a design method for a particular set of requirements consisting of a narrow range of input parameters is presented. The method uses an approximate linear theory with sheltering effect for resistance estimation and pressure distribution, and correlation with statistical analysis from the existing literature and the tank-test results available in the public domain. Though the optimisation of design parameters has been done for the design speed, but the resistance performance over the entire speed range has been incorporated in the design. The bulb behaviour has been discussed using the principle of minimisation of resistance and analysis of flow pattern over the bulb and near the sonar dome. It also explores the possible benefits arising out of new design from the production, acoustic, and hydrodynamic point of view. The results of this study are presented in the form of design parameters (for the bulbous bow) related to the main hull parameters for a set of input data in a narrow range. Finally, the method has been used to design the bulbous bow for a surface combatant vessel.

Keywords: Bulbous bow, hydrodynamic design, integrated bow, sonar dome, sheltering effect, wave resistance, naval ship, bulb behaviour

NOMENCLATURE

A_{BL}	Area of ram bow in longitudinal direction
A_{BT}	Cross-sectional area at forward (fwd) perpendicular (FP)
A_{MS}	Mid-ship sectional area
B_B	Maximum breadth of bulb area A_{BT}
B_{MS}	Breadth of ship at mid-ship
C_B	Block coefficient
C_M	Mid-ship coefficient
C_P	Prismatic coefficient
C_{PE}	Prismatic coefficient at the entrance
C_{WL}	Waterline coefficient
C_F	Frictional coefficient
C_R	Residual coefficient
$C_{P\nabla R}$	Residual power displacement coefficient
$\Delta C_{P\nabla R}$	Residual power displacement reduction coefficient
C_{ABL}	Lateral parameter

Revised 25 Feburary 2004

C_{ABT}	Cross-sectional parameter
C_{BB}	Breadth parameter
C_{LPR}	Length parameter
$C_{\forall PR}$	Volumetric parameter in percentage distributed fwd of FP
CFD	Computational fluid dynamics
C_{ZB}	Depth parameter
C_{CG}	Volumetric longitudinal distributional parameter
$C_{\forall BTOT}$	Volumetric parameter distributed aft and fwd of FP
Fn	$V_S / \sqrt{g . L_{LWL}}$ = Froude number
H	Mean draft of ship
B	Breadth of ship
H_1	H / L_{LWL}
H_B	Height of A_{BT}
k	$g . L_{LWL} / V_S^2$
L_E	Length of entrance
L_{LWL}	Length on load waterline
L_{PR}	Protruding length of bulb
μ, m	Doublet strength in + x or – x direction as per sign, and source distribution
ε_m	1 when m = 0, 2 when m = 1
P_D	Delivered
P_F	Frictional
P_R	Residual
P_{EF}	Effective frictional
P_{ER}	Effective residual power
ΔP_R	Residual power reduction factor
R	Ship's wave resistance
S_S	Ship's wetted surface
S_F	Ship's free surface
$\bar{S}_S$	Projection of S_S on the y = 0 plane
$\bar{S}_F$	Projection of S_F on the z = 0 plane
Re	$V_S . L_{LWL} / \nu$ = Reynolds number
V_S	Design speed of the ship
$\forall_{BTOT}$	Total bulb volume
$\forall_{PR}$	Protruding volume of bulb, fwd of FP
$\forall_{WL}$	Displacement volume of ship
ω	Tank width nondimensionalised by L_{LWL}
z_1	Submergence of point doublet
ε	B/L_{LWL}
Z_B	Height of the foremost point above keel line on the bulb at FP
η_D	Propulsive efficiency
ν	Kinematic viscosity of water
ρ	Density of water
g	Acceleration due to gravity

Superscript

Nondimensionalised by L_{LWL} denoted as $\bar{z}_1$

1. INTRODUCTION

R.E. Froude, who perhaps conceived a bulbous bow for the first time, had interpreted the lower resistance of a torpedo boat after fitting a torpedo tube as a wave reduction effect of the thickening of the bow. The protruding bulb form hydrodynamically affects the velocity field in the vicinity of the bow; in the region of rising bow wave. Primarily, the bulb attenuates the bow wave system, which results in a reduction of wave resistance with a properly designed bulb. Since the flow around the forebody

is smoothened, it may lead to reduction in the viscous resistance also. For fast ships, the use of a bulb allows a departure from the hitherto accepted design principles for the benefit of a better underwater form. Since, a suitably shaped and carefully designed bulb affects nearly all the hydrodynamic properties of a ship, it is important for the protruding bulb that the main parameters, ie, size ; volume distributed properly forward and aft of forward perpendicular; position and shape design for optimal performance subject to the constraint of the design. A properly designed bulbous bow reduces the resistance, but also enhances propeller cavitation characteristics, reduces fuel consumption, improves maximum speed and range, and may offer better housing for auxiliary sonar system.

The sonar domes are in use for a variety of naval ships, principally to house sonar transducers. These are located below the keel line of the ship, and in general, do not affect the wave-making resistance significantly. The design of a sonar dome is done mainly for size, volume, and location. Again, modern bulbous bows are appendages that are mainly designed for the improvement in ship's resistance, and are, in general, placed above the keel line and protrude longitudinally from forward (fwd) perpendicular (FP). The bulbous bow's nabla shape, location near the free surface, and the reduced size, volume, and breadth-to-height ratio are in direct contradiction to the geometry of the sonar dome located below the keel line.

Because of these reasons, recently the idea of bulbous bow has been extended from the commercial ships to the design of an integrated bow with a sonar dome for the naval ships[1,2]. In the present study, the detailed hydrodynamic design of the same idea has been investigated and a design method for an integrated bulbous bow that houses a sonar dome for the naval ships, has been presented. Though the main objective of the bulbous bow design is for the reduction in resistance, and hence less power, but there are other constraints that govern the final design of the integrated bulbous bow. Some of these constraints are: Effect on sonar dome performance, effect on hull structural elements, effect on anchor handling and other manoeuvring characteristics. Because of limited resources, a complete integrated design approach is beyond the scope of the present study. Hence in this study, mainly the design for resistance performance, and some other effects have been investigated using standardised tests and their interpretations.

Since the quantitative parameters are essential for the design of a bulb form, in theoretical accordance with the previous work[3], three linear and four nonlinear parameters have been used to describe and design the bulb form. These seven parameters are nondimensionalised with the ship particulars and are presented in decreasing order of importance. These are:

- C_{LPR} : It is the length parameter and defined as $C_{LPR} = L_{PR} / L_{LWL}$.
- C_{ABT} : It is the cross section parameter and defined as $C_{ABT} = A_{BT} / A_{MS}$.
- $C_{\forall PR}$: It is the volumetric parameter and defined in percentage as $C_{\forall PR} = \forall_{PR} / \forall_{WL} * 100$.

The volume $\forall_{PR}$ is distributed forward of FP. The total volume $\forall_{BTOT}$ is defined as the sum of $\forall_{PR}$ and fairing volume required aft of FP to fair the bulb in the ship. In the same manner, another volumetric coefficient is defined as $C_{\forall TOT} = \forall_{BTOT} / \forall_{WL}$.

- C_{CG} : It is volumetric distributional parameter that is LCG_B of the bulb volume as distributed (+ ve if located forward of FP and – ve if located aft of FP) divided by $(L_{WL} . Fn^2)$ of the ship $C_{CG} = LCG_B / (L_{WL} . Fn^2)$.
- C_{BB} : It is the breadth parameter and defined as $C_{BB} = B_B / B_{MS}$.
- C_{ZB} : It is the depth parameter and defined as $C_{ZB} = Z_B / H$.
- C_{ABL} : It is the lateral parameter and defined as $C_{ABL} = A_{BL} / A_{MS}$.

In the area of ship design in naval science, any design methodology is subjected to the following three stages.

Stage 1. *Preliminary hydrodynamic analysis*

This is CFD-based analysis. It deals with flow and performance characteristics (eg, resistance estimation, pressure distribution, flow pattern study with flow-field streamlines, velocity and wave profiles, etc). If the results are encouraging then the design proceeds to the next stage. If the results are not satisfactory, then based upon the CFD analysis, the design of the body is modified and the analysis is repeated till the results are satisfactory.

Stage 2. *Detailed hydrodynamic analysis*

This is typically done by model testing (eg, also referred to as tank testing). A model (ie, pre-selected one on a scale) is manufactured using some material and towed in a carriage tank to study and measure the flow and performance characteristics (eg, calm water resistance estimation, flow pattern study with paint flow test, image analysis of the photographs at various velocities, etc).

The results of the model testing are then extrapolated to full-scale for the ship using internationally accepted and standardised Froude's law of similarity, and International Towing Tank Conference (ITTC) 1957 Code of Practice.

Stage 3. *Full-scale sea trials*

Finally the designed ship is tested in actual conditions in sea/ocean/river/canal etc to confirm its performances as predicted by the model testing.

In the area of preliminary hydrodynamic analysis, a preliminary design method was discussed for a particular requirement consisting of a narrow range of parameters[4]. The method was tested on the designed bulb using numerical hydrodynamic computations. The flow and performance characteristics (eg, resistance estimation, pressure distribution, and flow pattern study with flow field streamlines), were studied for the designed integrated bulbous bow using CFD-based analysis. In the present study, based upon the results in the area of preliminary hydrodynamic analysis, the design methodology driven by model testing is being further investigated in detail.

Hence, the present study follows the previous one[4], but with the model-tested results. The present method uses an approximate linear theory with sheltering effect for resistance estimation and pressure distribution, and correlation with statistical analysis from the existing literature and tank-test results available in the public domain. The bulb behaviour over and near the sonar dome has been discussed using model-tested calm water resistance results, and other standardised tests; with one example of the integrated bulbous bow design for a surface combatant vessel.

2. LITERATURE REVIEW

Early studies to know the effect of bulbs on the hulls were carried out using experimental techniques on methodical series with Taylor bulbs[5-10]. Later, theoretically, the design of bulbous bow was studied using linearised theory of wave resistance[11]. Though the linearised theory gives a better understanding of the bulb action, it is still difficult to design the bulb for the given constraints due to lack of quantitative and qualitative guidelines. Again, a design procedure for the complete design (ie, size, location, and fairing to the hull, with qualitative and as well as quantitative guidelines) for a spherical bulb was discussed using linearised theoretical model[12]. Though the method gives an optimal bulb, there are other problems associated with the spherical bulbs (since for a sphere, the centre of gravity varies radially, the control of the bulb's centre of gravity is minimum, the surface of a sphere is highly non-developable, so the high production cost, and the fairing of a spherical bulb to the hull is difficult for both *U* and *V*-shaped forebodies). This work[12] was extended further to study the effect of sheltering on a spherical bulb[13]. The variation of optimum location for the bulb for various types of ships (ie, sine ship, cosine ship, and parabolic ship)[13] has also been presented.

The first quantitative and comprehensive design method was discussed using a statistical method derived from an analysis of propulsion tests[3,14]. The method gives design parameters for a selected bulb, for a selected ship, with a flexibility of choosing power reduction factor. In this method[3,14], some linear and nonlinear parameters for the bulb were

chosen as the design parameters. Though the parameters were sufficient to design a bulb, these did not produce direct guidelines for the location of the centre of gravity of the bulb. It may be argued that the selection of the parameters will affect the centre of gravity, but specifying an optimal location will serve better for the design. Since the method is based upon the model test results, it gives fairly good preliminary guidelines for the design of the bulb. But since, as per the wave resistance minimisation theory, the amplitude (a function of the mass or size of the bulb) and phase difference (a function of the centre of gravity of the underwater distributed volume of the bulb) of the bulb's wave pattern ultimately affect the wave resistance, so the location is to be chosen carefully.

In the recent years, efforts have been made in the area of CFD to optimise hull forms with bulbous bows. The idea is to study the flow characteristics of a variation of hull forms using CFD and searching for the optimal hull using computational tools. This has one distinct advantage: it reduces the number of tank tests. The various authors have presented investigations on the design of integrated bulb with the existing sonar dome, using CFD optimisation and a number of tank tests[1,2,15,16]. In the various studies[1, 2, 15,16] on CFD analysis, the performances of various bulbs have been discussed, but not the design procedure or how to get the basic shape of hull or bulb. In CFD optimisation when one is searching for the optimal solution in a domain consisting of fixed discrete values, the starting point (or first basic option upon which successive modifications are carried out) is important not only from a computational point of view but also because it decides the validity of the final solution. It is to fill this gap that the present study has been carried out.

3. HYDRODYNAMIC DESIGN

3.1 Reanalysis of Statistical Data

In theoretical accordance with the earlier work[3], a power reduction factor or the bulb's effect on power is defined as

$$\Delta P = 1.0 - (P_W / P_O)$$

where P_W is the power with the bulb and P_O is the power without the bulb. In accordance with the Froude method, the resistance separation for ships without bulb or with the bulb is:

$$P_T = P_R + P_F$$

The residual power P_R can be calculated with a known propulsive efficiency η_D, as the difference between the total power P_T and the frictional power P_F, and a residual power reduction factor obtained as

$$\Delta P_R = 1.0 - (P_{RW} / P_{RO})$$
$$= 1.0 - (P_{DW} - P_{FW}) / (P_{DO} - P_{FO})$$

Using the ITTC (1957) Code of Practice, for friction line and η_D, the residual power reduction is:

$$\Delta P = 1.0 - \left(\frac{P_{DW}\cdot\eta_{DW} - P_{EFW}}{P_{DO}\cdot\eta_{DO} - P_{EFO}}\right)\cdot\left(\frac{\eta_{DO}}{\eta_{DW}}\right)$$

Though the propulsive efficiency is different for ships with the bulb or without the bulb, for simplification, a constant value $\eta_{DW} = \eta_{DO}$ has been assumed. In general, for additive bulbs:

$$P_{EFW} > P_{EFO} \text{ because } S_W > S_O$$

and

$$P_{DW} < P_{DO}$$

$$\eta_{DW} > \eta_{DO}$$

and

$$P_{DW}\cdot\eta_{DWn} > P_{DW}\cdot\eta_{DO}$$

consequently

$$P_{DW}\cdot\eta_{DW} - P_{EFW} > P_{DO}\cdot\eta_{DO} - P_{EFO}$$

since $\left(\frac{\eta_{DO}}{\eta_{DW}}\right) < 1.0$

it follow:

$$\left(P_{DW}.\eta_{DW} - P_{EFW} \right).\left(\frac{\eta_{DO}}{\eta_{DW}}\right) \approx \left(P_{DW}.\eta_{DO} - P_{EFW}\right)$$

Herein, the residual power reduction factor used is:

$$\Delta P_R = 1.0 - \left(P_{DW} - P_{EFW}/\eta_D\right)/\left(P_{DO} - P_{EFO}/\eta_D\right)$$

In general, the propulsive efficiency is not given for all the data available, therefore in this study, a constant value of η_D has been assumed. In the C_B range of 0.500–0.525, a value of 0.7 can be assumed safely. The change in η_D of $\pm$ 3.0 per cent affects the $\Delta C_{P\nabla R}$ by only $\pm$4.0 per cent at low Froude numbers, and at higher Froude numbers, the change is $\pm$1.5 per cent[14]. Since the study was mainly concentrated in the low range of Froude number, the assumption of constant η_D is justified. To eliminate the effect of ship hull form, a dimensionless power displacement coefficient is defined as

$$C_{P\nabla} = P/\left(\rho/2V_S^3.\forall_{WL}^{2/3}\right)$$

This leads to the residual power coefficient

$$C_{P\nabla R} = P_D/\left(\rho/2V_S^3.\forall_{WL}^{2/3}\right) - C_F S/\left(\eta_D.\forall_{WL}^{2/3}\right)$$

with C_F according to the ITTC (1957) Code of Practice, for friction line and to the bulb effect related to the residual power coefficient, that is to the residual power reduction coefficient (neglecting the form factor k), one has:

$$\Delta C_{P\nabla R} = 1.0 - C_{P\nabla RW}/C_{P\nabla R}$$

The residual power reduction coefficient can be scaled directly to the full-scale ship. The low sea-wave influence on full-scale measurement is eliminated. Though the amounts do not match similarly but this may be because of the two different trims in with or without bulb form, and it hardly affects the residual power reduction coefficient. In this study, the bulb parameters (ie, C_{LPR}, C_{ABT}, $C_{\forall PR}$, $C_{\forall TOT}$, C_{BB}, and C_{ABL}) have been derived by nonlinear multivariate regression analysis from the experimental data available in the public domain[7,8,10,14,17], and the tests were conducted at the Ship Hydrodynamics Laboratory, Dept of Ocean Engineering and Naval Architecture, IIT Kharagpur. The analysis has been done for maximum and relatively constant (ie, 0.35–0.45, discrete maximum error = 10 %) $\Delta C_{P\nabla R}$ and in a narrow range of ship particulars (ie, C_B= 0.500–0.525, C_{WL}= 0.79–0.85, C_M= 0.87–0.99, C_{PE}= 0.65–0.73, L_{WL}/B = 5.20–7.55, B/H = 2.15–3.15, L_E/B = 2.05–3.80, and Fn = 0.170–0.385). The results have been presented in a narrow range (ie, C_B = 0.500 and 0.525 and Fn = 0.170–0.385). The nonlinear multivariate regression analysis[18,19] has been done with NRLEG™* software (version 5.3) and the results have been plotted in Microsoft EXCEL™**. The results are given in Figs 1 to 4, and 6 to 8, for parameters* C_{LPR}, C_{ABT}, $C_{\forall PR}$, $C_{\forall TOT}$, C_{BB}, and C_{ABL}.

3.2 Reanalysis of Sheltering Effect

The basic assumption in the Michell's theory[21] is that the ship is thin and flow perturbations due to the ship are related only to the ship's beam/length ratio $\varepsilon = B_{MS}/L_{LWL}$. This is particularly not true for $\varepsilon > 0.1$; the effect of breadth-length ratio on resistance is known as sheltering effect[12]. For higher values of ε, this effect is complicated by mutual interferences of the thinness parameter ε,

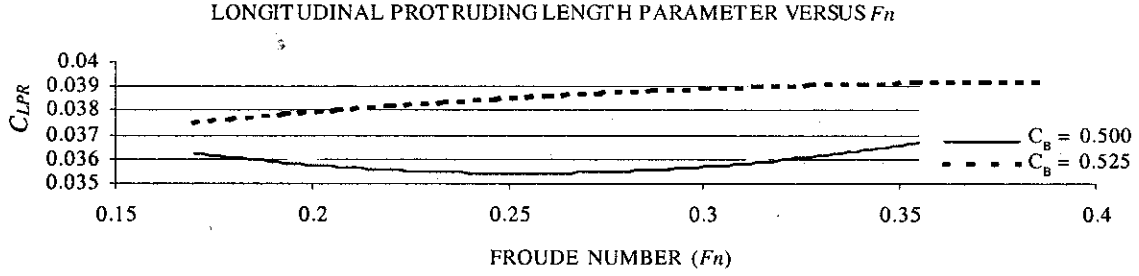

Figure 1. Variation of longitudinal length parameter for Froude number and block coefficient

* The separate detailed discussion on individual parameters can be found in other works[4,20].

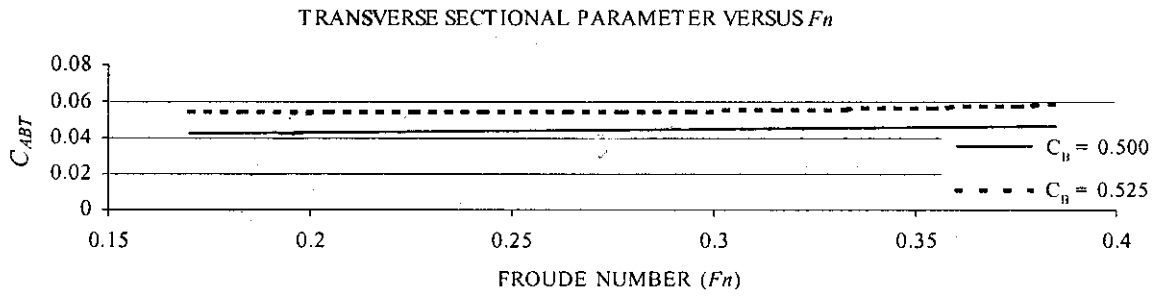

Figure 2. Variation of transverse cross-sectional parameter for Froude number and block coefficient

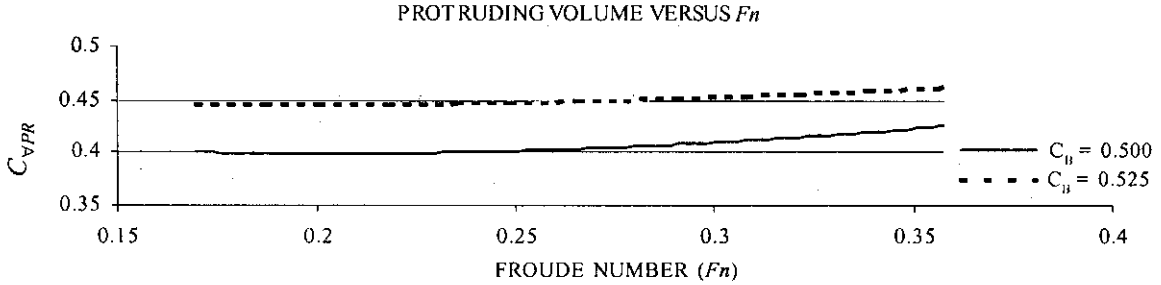

Figure 3. Variation of protruding volume parameter for Froude number and block coefficient

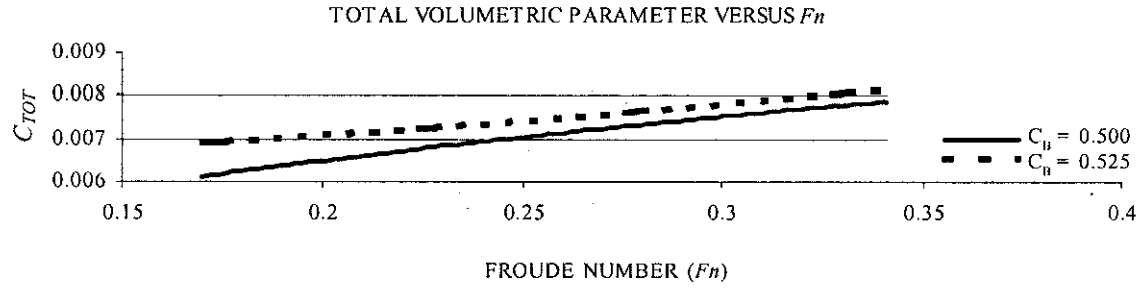

Figure 4. Variation of total volume parameter for Froude number and block coefficient

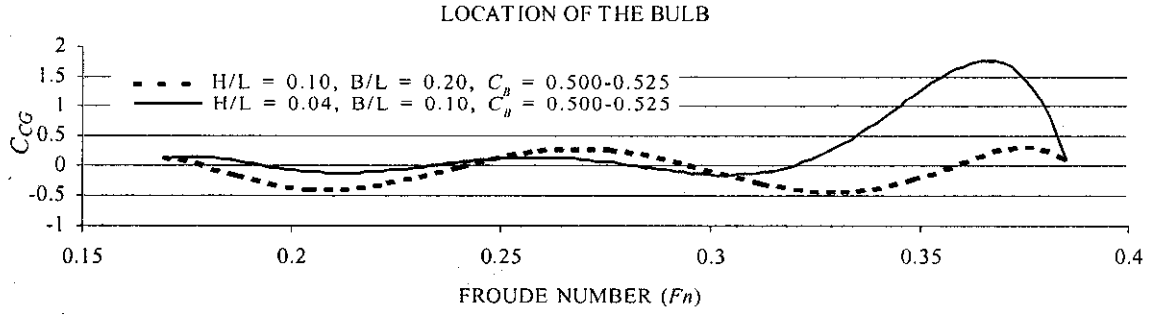

Figure 5. Variation of location of CG of the bulb for Froude number and block coefficient

the wave number k, and the boundary layer thickness. A theory has been developed for the sheltering effect on the ship-wave resistance, treating the problem by free-surface distribution inside the ship[13]. Though there are other theories also to incorporate the sheltering effect, but these have not been proved

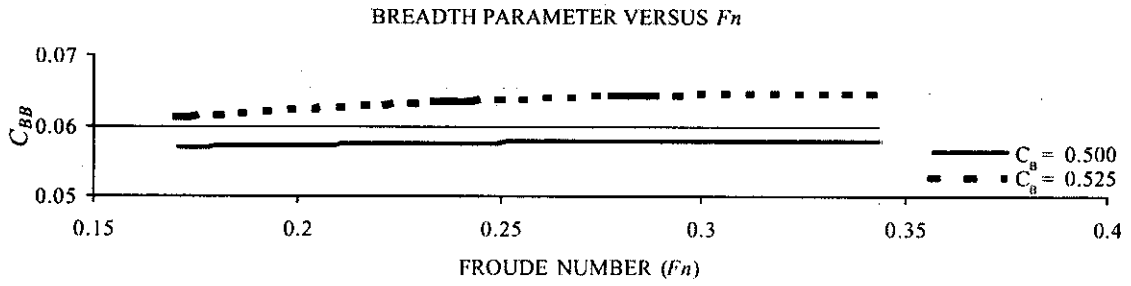

Figure 6. Variation of breadth parameter for Froude number and block coefficient

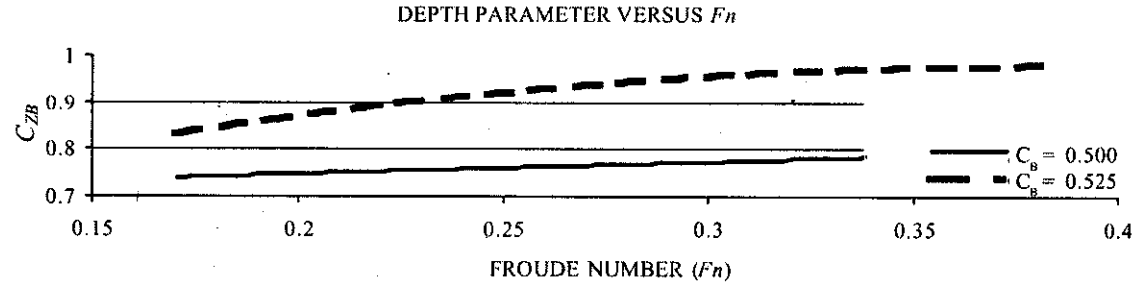

Figure 7. Variation of the depth parameter for Froude number and block coefficient

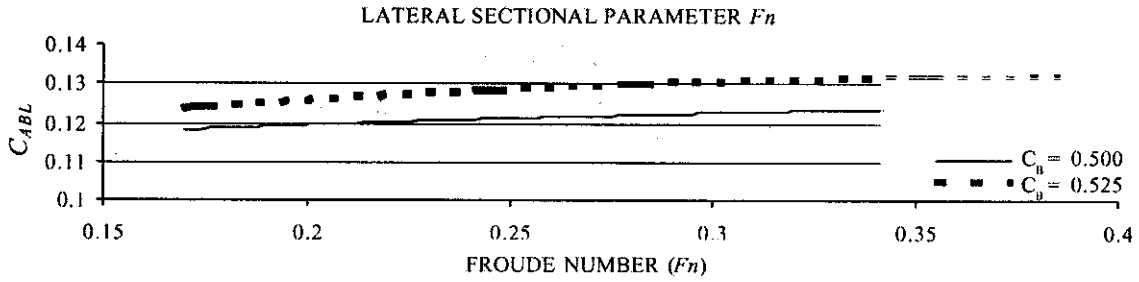

Figure 8. Variation of lateral parameter for Froude number and block coefficient

to be satisfactory experimentally[13,14]. In this study, an approximate solution of Yim's theory[13] has been used to drive the design charts for C_{CG}. In theoretical accordance with Yim's theory[13], and following the conventions defined in Fig. 9, for numerical computations, the wave resistance[12,22] is given by

$$\frac{R}{\frac{\rho}{2}V_S^2 L_{LWL}^2} = \frac{16\pi^2 k}{\omega}\sum_{m=0}^{\infty}\varepsilon_m \frac{1+\sqrt{1+\left(\frac{4\pi m}{k\omega}\right)^2}}{\sqrt{1+\left(\frac{4\pi m}{k\omega}\right)^2}}\left(P^2+Q^2\right)$$

where

$$P+iQ = \iiint_D \sigma(x,y,z)\exp\left\{kb(zb+ix)+i z\pi y\frac{m}{\omega}\right\}dD$$

$$b = \left[\frac{1}{2}+\frac{1}{2}\left\{1+\left(\frac{4\pi m}{k\omega}\right)^2\right\}^{1/2}\right]^{1/2}$$

and ω= Width of the towing tank nondimensionalised by ship length, L_{WL}.

$\varepsilon_0 = 1$, $\varepsilon_m = 2$ for $m \geq 1$, D = Domain of source distribution, and $\sigma = \sigma_0 + \sigma_F$.

The introduction of a towing tank is just for the convenience of numerical computation. It is known

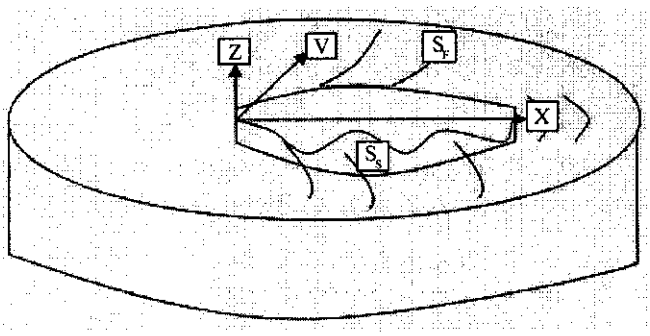

Figure 9. Schematic diagram for a surface ship and coordinate system.

that the wave resistance[12] at $\omega = 5$ is already equal to $\omega = \infty$.

Again for simplification,

$$P + iQ = Q_0\left\{\sin(kb)\frac{kb}{k^2b^2-\pi^2} + i\frac{kb(\cos kb+1)}{k^2b^2-\pi^2}\right\} - ikb\mu\exp\left(-kb^2\bar{z}_1\right)$$

where

$$Q_0 = \frac{\overline{B}}{2kb^2}\left[\begin{matrix}1-\left(1-\beta\overline{H}\right)\exp\left(-kb^2\overline{H}\right)\\ -\frac{\beta}{kb^2}\left\{1-\exp\left(-kb^2\overline{H}\right)\right\}\end{matrix}\right]$$

The bow resistance comes only from

$$Q_1 \equiv Q_0\frac{kb}{k^2b^2-\pi^2} + kb\mu\exp\left(-kb^2\bar{z}_1\right)$$

The optimum μ is derived from minimising the total wave resistance

$$\frac{\partial R}{\partial \mu} = 0$$

or

$$\mu = \frac{\sum_{m=0}^{\infty}\varepsilon_m\frac{2b^2}{2b^2-1}Q\frac{kb^2(\cos kb+1)}{k^2b^2-\pi^2}\exp\left(-kb^2\bar{z}_1\right)}{\sum_{m=0}^{\infty}\varepsilon_m\frac{2b^2}{2b^2-1}b\exp\left(-2kb^2\bar{z}_1\right)} \quad (1)$$

which includes the effect of the stern.

With the given values of source distribution, P, Q etc (ie, for sine ship, cosine ship or parabolic ship[12,23]), the Eqn (1) can be solved, exactly. Again, using the principle of superimposition, a ship can be represented as a combination of various sine, cosine, or parabolic hulls, for which the exact formulas are given. Though the exact solution of Eqn (1) is possible, in this study, the Eqn (1) has been solved approximately. To approximate the solution function for optimum location, it has been assumed that the optimum location is a function of only H/L_{LWL}, B/L_{LWL}, and z/H_1 in the range C_B = 0.500–0.525, hence, neglecting the complexities. Since the solution for Eqn (1) is a periodic function, the approximation theory of periodic functions has been used to determine the approximate solution[24,25]. Assuming a point doublet located near the bow stem at a typical depth of z/H_1 = 0.75–0.85 (ie, for C_B = 0.500–0.525, and Fn = 0.18–0.40, which is a fair approximation as per the existing practices), the approximate optimum location of the bulb (ie, bulb parameter C_{ZB}) was derived. It has been presented in Fig. 5. In general, the waterlines of a ship are not similar to waterlines of sine ship, cosine ship or parabolic ship. However in specific cases, a multivariate function (ie, a function of sine, cosine, and parabolic distributions) fitting the waterlines can be assumed safely[13]. Accordingly, a decision regarding the longitudinal centre of buoyancy of the bulb (LCG_B) can be taken.

4. EXAMPLE

A bulbous bow is to be designed for the Navy destroyer#. The ship particulars are:

L_{BP} = 161.239 m

L_{LWL} = 165.200 m

D = 10.668 m

H_{FP} = 6.669 m

H_{AP} = 6.669 m

$H = (H_{AP} + H_{FP})/2$ = 6.669 m

$B = B_{MS}$ = 16.794 m

This is classified defence Naval ship; hence because of copyright, other details(ie, sectional area curves, etc) cannot be given here.

$\Delta = (\forall_{WL} * \rho_{seawater}) = 9532.703$ ton

$A_{MS} = 108.136$ m^2

$C_B = 0.515$ at 6.669 m draft

$V_S = 22$ knot

$Fn = 0.281$

at the design speed.

From the Figs 1–8, the design particulars for the bulbous bow are:

$C_{BB} = 0.063175$ and $B_B = 1.060$ m

$C_{LPR} = 0.0370$ and $L_{PR} = 6.114990$ m

$C_{ZB} = 0.9375$ and $Z_B = 6.2520$ m

$C_{ABT} = 0.0550$ and $A_{BT} = 5.9500$ m^2

$C_{ABL} = 0.1200$ and $A_{BL} = 12.9760$ m^2

$C_{\forall PR} = 0.4375$ % and $\forall_{LR} = 40.6600$ m^3

$C_{\forall TOT} = 0.0075$ and $\forall_{TOT} = 69.6980$ m^3

$C_{CG} = (-0.0150)$ and $LCG_B = (-0.1950$ m, ie, 0.1950 m from FP towards AP).

Because of production and fairing constraints, from the design point of view, it is difficult to design a bulb strictly satisfying all the values given above, therefore some adjustments have been implemented. The opening at the integrated bow has been elongated and the longitudinal centre of buoyancy of the bulb brought further forward towards FP.

The integrated bulb is of additive type rather than implicit type with a sharp chine line (line of C^0 continuity), and has nabla shape (ie, top heavy inverted-onion shaped). Furthermore, the opening is conical in shape, with sections having a mix of straight and circular shapes. The integrated designed bulb has higher values (3–5 %) of L_{PR}, A_{BT}, A_{BL}, and $\forall_{LR}$ than given above. In this process of fairing of integrated bulbous bow into the parent ship, the sections between 8th–10th stations will alter slightly with an addition of cross-sectional area, and longitudinal centre of bouyancy will move forward (ie, 0.478 %) from its original position for the parent ship.

After adjustments, the design particulars for the designed integrated bulbous bow are:

$B_B = 1.0600$ m

$L_{PR} = 6.4055$ m

$Z_B = 6.2520$ m

$A_{BT} = 6.2475$ m^2

$A_{BL} = 13.6248$ m^2

$\forall_{LR} = 42.6930$ m^3

$\forall_{TOT} = 73.1829$ m^3

$LCG_B = -0.1800$ m (ie, 0.1800 m from FP towards AP).

The model testing has been done with both the cases, ie, the Navy destroyer ship without integrated bulbous bow, and with integrated bulbous bow. The basic details about the model testing, and the models have been presented in Table 1.

The images of the models for the Navy destroyer ship without and with integrated bulbous bow have been shown in Figs 10 and 11. The resistance in calm water flow has been tested over a speed range 14.0–30.0 knot including the design speed, for both the cases. Again for both the cases, the hydrodynamic properties have been tested only at

Table 1. Details about the model testing

Properties	Navy destroyer ship without integrated bulbous bow	Navy destroyer ship with integrated bulbous bow
Scale ratio	30	30
Model material	FRP	FRP
Type of tests	Calm water resistance test, paint flow test, and images of the flow around bow region at various speeds	Calm water resistance test, paint flow test, and images of the flow around bow region at various speeds

the design speed. The results for the Navy destroyer ship have been presented. The test results** are presented as a comparative study because at higher speeds, the test results show good agreement with the full-scale sea trials[26].

Figures 12 and 13 show the tested flow direction (via image analysis of flow field streamlines using paint flow test, and superimposed over the flow-field streamlines computed with numerical hydrodynamics[4]) over the sonar dome without the bulbous bow and with the bulbous bow, respectively. It is clear from the two figures that there are two origins of flows: One originating at the opening of the bulb, and the other at the tip of the sonar dome. The flow-field streamlines show that these two flows are different in nature, and the flow originating at the opening of the bulb is not affecting the flow over the sonar dome. Furthermore, it was also shown using numerical computations that there is no significant change in the pressure distribution over the sonar dome due to the presence of the bulbous bow (ie, the zone that is important[4]). Again, the directions of change in pressure gradients are different for flows originating at the integrated bulbous bow's opening, and at the tip of the sonar dome; hence the two flows are different in nature and are not affecting each other adversely because of sensitive sensor location in that area[1,20].

Figure 14 shows the image of the flow around integrated bulbous bow at the design speed. The image shows that the flow originating at the bulbous bow rises upwards with some intermixing of flow, but is well above the sonar dome. Hence, any rising of wave originating at the bulb basically moves upwards and in a different, and safe direction from the sonar point of view. In addition, since

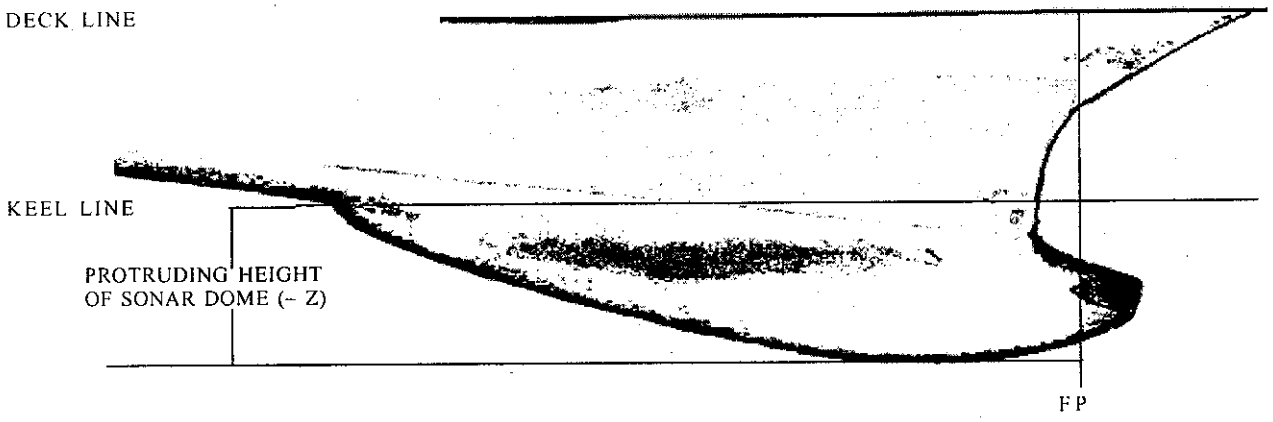

Figure 10. Image of a model of the Navy destroyer ship without integrated bulb

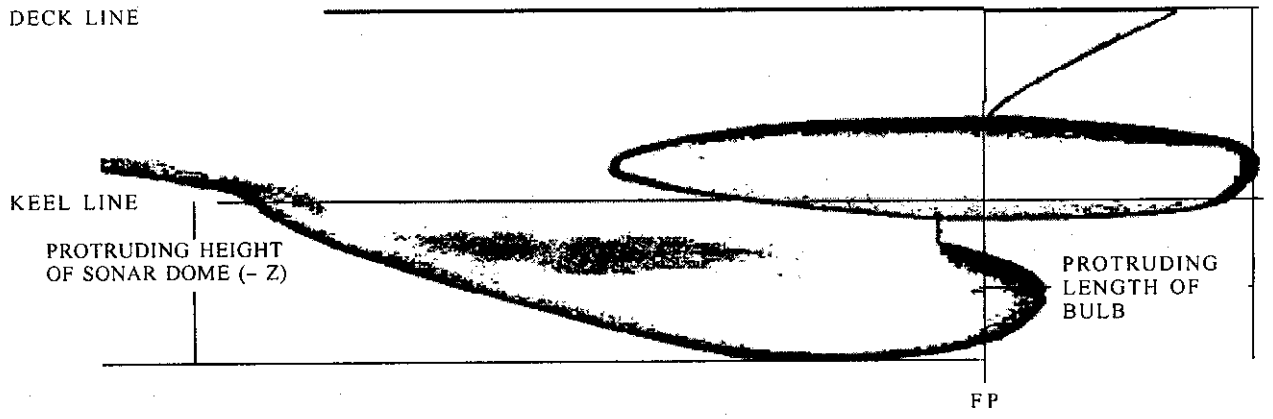

Figure 11. Image of a model of the Navy destroyer ship with designed integrated bulbous bow

**However, all the test results are not given here. The details for the complete test results can be found in other research work[20].

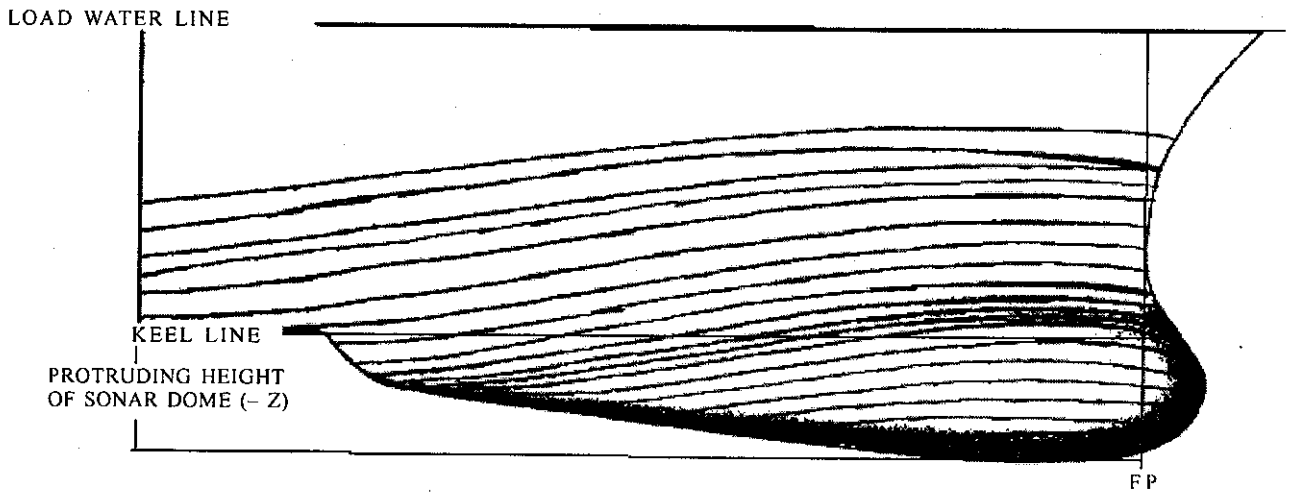

Figure 12. Model tested flow-field streamlines over the bow region without design bulb

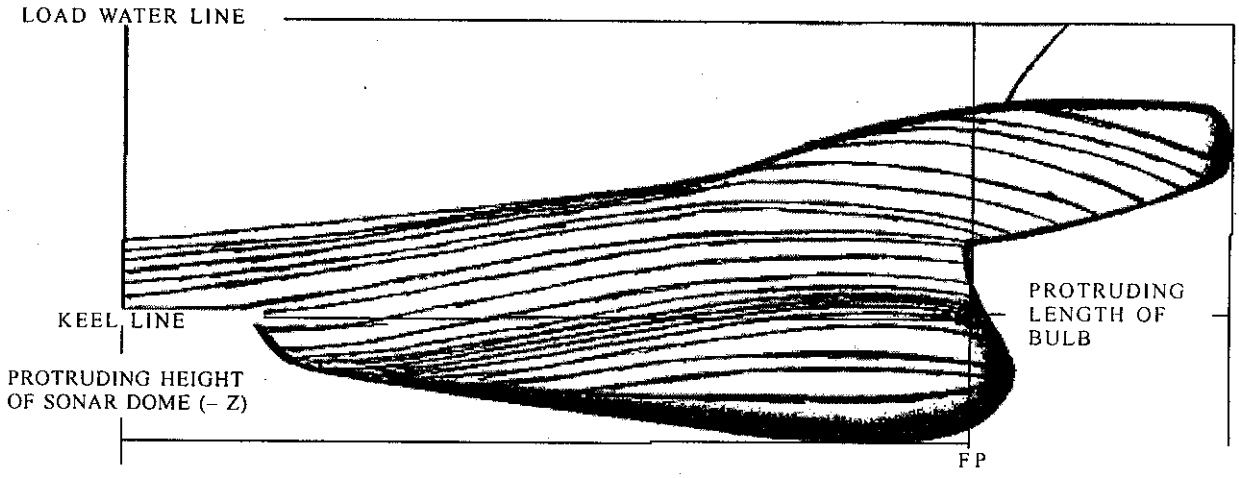

Figure 13. Model-tested flow-field streamlines over the bow region with design bulb

the change of pressure gradients are different, intermixing of flows is away from the sonar dome, and the movement of wave originating at the bulb is upwards; it can be concluded that there shall not be any addition of noise, or significant alteration in the noise pattern, around the sonar dome. However, this is a preliminary analysis as far as the noise pattern around the sonar dome is concerned. It has to be studied further using numerical modelling, suitably supported by standardised tests, to determine the noise pattern around the sonar dome in the case of integrated bulbous bow for the Navy destroyer ship.

The results of calm water resistance tests are shown in Fig. 15. In addition, the numcrically computed result[4], has also been shown in Fig. 15, for a comparative study. The nature of the model-tested resistance ratio curve in Fig. 15, at 6.669 m draft shows that the minimisation is working at this draft. Furthermore, it can be seen from the Fig. 15, that the maximum resistance reduction of 6.9525 per cent is occurring at Fn = 0.2874 (ie, 22.5 knot) as compared to the design Fn of 0.28106 (ie, 22.0 knot), (ie, error margin = 2.2727 %, and that is less than the discrete maximum error of 10 % as described in the Section 3.1).

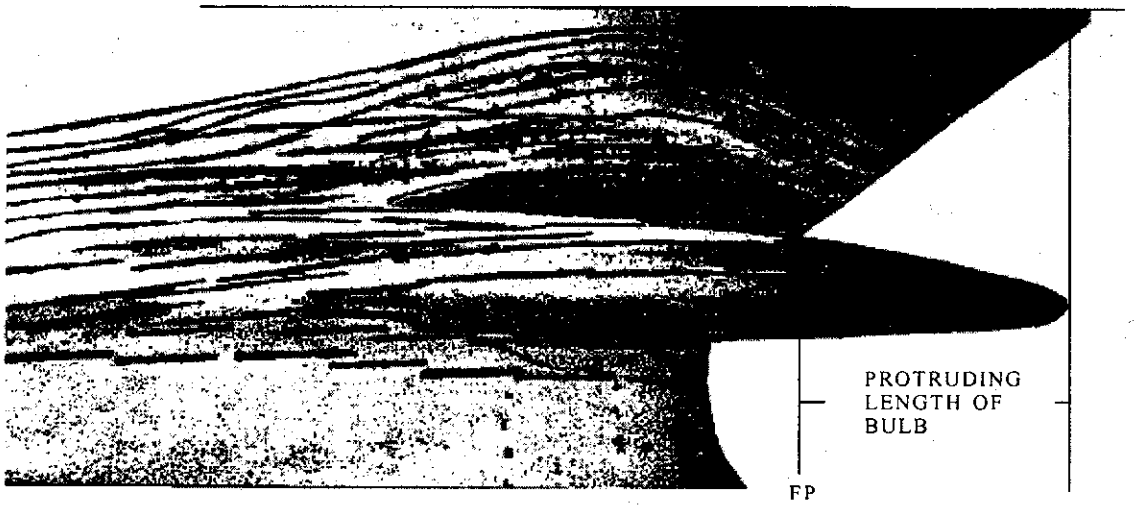

Figure 14. Image of the flow around designed integrated bulbous bow at the design speed

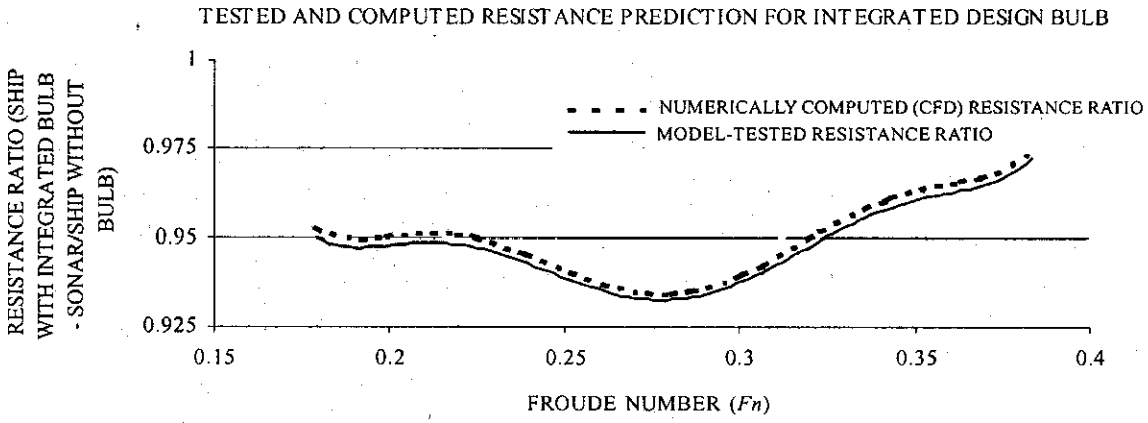

Figure 15. Model-tested resistance ratio of the integrated bulbous bow

Again, from Fig. 15, it is clear that the model-tested resistance is less with the integrated bulb than without the bulbous bow, over the entire considered range(ie, $Fn = 0.17885–0.38326$, or 14.0–30.0 knot). Using constant cost life-cycle analysis, this resistance ratio will mean a drop in fuel consumption (3.576 %), increase in speed range (3.852 %), and increase in maximum operating speed (0.161 knot). And, since the resistance of the ship with the integrated bulb, is less than the resistance of the ship without the integrated bulb, it will mean that in the case of ship with integrated bulb, the propeller cavitation characteristics will improve considerably. Furthermore, the enhanced volume, space, and area provided by the integrated bulb may be utilised to house other sensing systems. A comparative analysis between CFD-based preliminary analysis[4], and model-tested results is shown in Table 2.

5. CONCLUSIONS

The investigations on a design method for integration of an existing bow that houses a sonar dome, in a narrow range of parameters have been presented. In the curves, the behaviour and the effect of the hull parameters on the bulb design have been shown. However, the authenticity of the curves has not been studied exhaustively, confirming to model testing. Furthermore, the design curves have been derived for maximum and relatively constant ΔC_{PVR}, and

Table 2. Comparative analysis between CFD-based preliminary analysis[4] and model-tested results

Results of less resistance on other characteristics	CFD-based preliminary analysis[4]	Results of model testing
Drop in fuel consumption (%)	3.500	3.576
Increase in overall speed range (%)	3.770	3.852
Increase in maximum operating speed (knot)	0.158	0.161

in a narrow range of ship particulars. An obvious extension shall be to derive the design curves for predetermined lower and upper bounds of ΔC_{PVR} and in broader range of ship particulars; to utilise the design methodology in the area of CFD-based shape optimisation of integrated bulbous bow, and ships.

The optimisation of design parameters has been done for the design speed only, but the performance over the entire speed range has been incorporated in the design. Since the design procedure has been discussed in a narrow range, the curves can be used for detailed hydrodynamic design of a bulb for a single-draft ship with caution. The advantages of the integrated bulb for a ship with sonar dome and various additional opportunities that the new combination might offer, have been presented.

One design example of an integrated bulbous bow has been discussed for the Navy destroyer ship with the model-tested results. Since, the results of this study are encouraging and the potential benefits with the full utilisation of the new design are significant, this study can be extended to a complete and thorough study to design the integrated bulb, with CFD optimisation and sea-trial tests, incorporating detailed investigation on other aspects of the integrated bulb (ie, cavitation on the bulbous bow, flow noise, buoyancy and trim effects of hull, intact and damaged dynamic stabilities, low and high speed manoeuvring and seakeeping, and vibration studies).

6. TRADEMARKS & COPYRIGHTS

The NRLEG™ software (version 5.3), trademark and copyright © 1992-2002, with Phillip H. Sherrod, USA. The Microsoft EXCEL™, trademark and copyright, with Microsoft Corporation, USA.

ACKNOWLEDGEMENTS

The authors are thankful to Prof (Retd) R.P. Gokarn for his valuable comments and suggestions, which have helped immensely in revising the manuscript. The authors are also thankful to Dr M. Ghosh (Postdoctoral Fellow, Dept of Mathematics, University of Torento, Italy) and Ing. G. Chiandussi (Dept of Mechanical Engineering, Technical University of Turin, Torino, Italy) for their help in model-related testing and analysis.

REFERENCES

1. Cusanelli, D.S. Development of a bow for a naval surface combatant which combines a hydrodynamic bulb and a sonar dome. *In* American Society of Naval Engineers, Technical Innovation Symposium, 1994. pp. 231-47.
2. Cusanelli, D.S. & Karafiath, G. Combined bulbous bow and sonar dome for a vessel. US Patent No. US 52,80,761, 1994.
3. Kracht, A.M. Design of bulbous bows. *SNAME Transactions*, 1978, **86**, 197–17.
4. Sharma, R. A preliminary investigation on hydrodynamic design of integrated sonar dome and bulbous bow for naval ships. *In* Proceedings of the International Conference on Sonar-Sensors and Systems, ICONS–2002, edited by H.R.S. Sastry, D.D. Ebenezer and T.V.S. Sundaram. Allied Publishers Ltd, New Delhi, India. pp. 941–54. ISBN 81-7764-381-9
5. Taylor, D.W. *In* Marine engineering and shipping age, 1923. pp. 540-48.
6. Bragg, M. Results of experiments upon bulbous bows. *SNAME Transactions*, 1930, **38**, 33-56.
7. Ferguson, J.M. & Parker, M.N. Model resistance tests on a methodical series of forms. *Transactions RINA*, 1970, **98**(1), 1–30.
8. Ferguson, A. M. Hull and bulbous bow interaction, *Transactions RINA*, 1967, **95**, 421–41.

9. Inui, T.; Takaehi, T. & Kumano, M. Wave profile measurement on the wave-making characteristics of the bulbous bow. *In* Society of Naval Architects of Japan (Translation from the University of Michigan), 1960. pp. 14-25

10. Muntjewerf, J.J. Methodical series experiments on cylindrical bows. *Transactions RINA*, 1967, **95**, 199–23.

11. Yim, B. On the wave resistance of surface-effect ships. *J. Ship Research*, 1971, **15**(3), 22-32.

12. Yim, B. A simple design theory and method for bulbous bows of ships. *J. Ship Research*, 1974 **18**(3), 141-52.

13. Yim, B. Simple calculation of sheltering effect on ship-wave resistance and bulbous bow design. *J. Ship Research*, 1980, **24**(4), 232-24.

14. Kracht, A.M. weitere Untersuchungen über die Anwendung von Bugwülsten, VWS Bericht No. 811/78, Berlin, 1978. (in German).

15. Cusanelli, D.S.; Jessup, S.D. & Gowing, S. Exploring hydrodynamic enhancements to the USS Arleigh Burke (DDG-51). *In* Proceedings of the Fifth International Conference on Fast Sea Transportation (FAST'99), Seattle, WA, August 1999. pp. 123-36.

16. Cusanelli, D.S.; Jessup, S.D. & Gowing, S. Performance of near-surface bow bulbs in irregular waves. *In* Proceedings of the 25th ATTC, Iowa City, 1998.1. pp. 61-70.

17. PR. Graduate student's project report, Institute of Naval Architecture, Marine and Ocean Engineering, Technical University of Berlin, Berlin, 1998. 1–86 (in German).

18. Kachigan, S.K. Multivariate statistical analysis: A conceptual introduction. Radius Press, 1991. ISBN: 0942154916

19. Bates, D.M. & Watts, D.G. Nonlinear regression analysis and its applications. Wiley Series in Probability and Mathematical Statistics. John Wiley and Sons, 1988. ISBN: 0471816434

20. Sharma, R & Sha, O.P. Design investigation on integrated bulbous bows for naval ships. *In* Department of Ocean Engineering and Naval Architecture, Indian Institute of Technology, Kharagpur, India, 2003. Project Report PR–4/2003.

21. Michell, J.H. The wave resistance of a ship moving. *Philosophical Magazine*, 1898, **45**, 22-29.

22. Srettensky, L.N. On the wave-making resistance of a ship moving in a canal. *Philosophical Magazine*, 1936, **22**, 7th Series.

23. Inui, T.; Takaehi, T. & Kumano, M. Wave profile measurement on the wave-making characteristics of the bulbous bow. *In* Society of Naval Architects of Japan (Translation from the University of Michigan, 1960). pp. 46-58.

24. Temlyakov, V.N. Approximation of periodic functions. *In* Series in Computational Mathematics and Analysis. Nova Science Publishers Inc, November 1993. pp. 55-78. ISBN:1560721316

25. Stepanets, A.I. Classification and approximation of periodic functions. *In* Series in Mathematics and its Applications, Vol. **333**, Kluwer Academic Publishers, 1995. pp. 178-241. ISBN: 0792336038

26. Hoyle, J.W.; Cheng, B. H.; Hays, B.; Johnson, B. & Nehrling, B. A bulbous bow design methodology for high-speed ships. *SNAME Transactions*, 1986, **94**, 19-28.